Trovacene Chemistry. 10 [1]
The [1]- and [2]Silatrovacenophanes (η^7-C_7H_6)V(η^5-$C_5H_4SiR_2$) and (η^7-C_7H_6)V(η^5-$C_5H_4SiR_2SiR_2$ (R = Me, Ph): Synthesis, Structure, and Ring Opening

Christoph Elschenbroich*, Francesca Paganelli, Mathias Nowotny, Bernhard Neumüller, and Olaf Burghaus

Marburg, Fachbereich Chemie der Philipps-Universität

Received June 18th, 2004.

Dedicated to Professor Albrecht Salzer on the Occasion of his 60th Birthday

Abstract. Heteroannular dilithiation of trovacene, (η^7-C_7H_7)V(η^5-C_5H_5) (**1•**), and subsequent reaction with the respective dichlorosilane yielded the [1]silatrovacenophanes (η^7-C_7H_6)V(η^5-$C_5H_4SiR_2$) (**2•**, R = Ph; **3•**, R = Me) and the [2]silatrovacenophane (η^7-C_7H_6)V(η^5-$C_5H_4SiMe_2SiMe_2$) (**4•**). Structural studies by X-ray diffraction revealed sandwich tilt angles of 17.3° (**2•**) and 3.8° (**4•**), respectively, and considerable strain in the ring-link-ring region. EPR spectroscopy responds to these distortions in that the g-tensor is tetragonal ($g_x = g_y \neq g_z$) for **4•** but rhombic ($g_x \neq g_y \neq g_z$) for **2•** and **3•**. With increasing tilt, <g> increases slightly towards g_{fs} = 2.0023 and a(^{51}V) decreases, the latter response to tilting being more pronounced. These trends are plausible in view of distortion-induced mixing of the V($3d_{z^2}$) SOMO with ligand π orbitals. Whereas cyclic voltammetry of undistorted **4•** displays reversible oxidation and reduction, the strained sandwich **2•** shows irreversible behavior, probably caused by cleavage of the interannular bridge. [1]Silatrovacenophanes are thermally more robust than [1]silaferrocenophanes in that **2•**, exposed to 280 °C, fails to show indications of ring-opening polymerization (ROP).

Keywords: Metallocenophanes; Mixed-ligand sandwich; EPR-spectroscopy; Cyclic voltammetry; Ring-opening polymerization

Trovacenchemie. 10 [1]
Die [1]- und [2]Silatrovacenophane (η^7-C_7H_6)V(η^5-$C_5H_4SiR_2$) und (η^7-C_7H_6)V(η^5-$C_5H_4SiR_2SiR_2$ (R = Me, Ph): Synthese, Struktur und Ringöffnung

Inhaltsübersicht. Heteroannulare Dilithiierung von Trovacen, (η^7-C_7H_7)V(η^5-C_5H_5) (**1•**), und anschließende Reaktion mit den entsprechenden Dihalogensilanen lieferte die [1]Silatrovacenophane (η^7-C_7H_6)V(η^5-$C_5H_4SiR_2$) (**2•**, R = Ph; **3•**, R = Me) und das [2]Silatrovacenophan (η^7-C_7H_6)V(η^5-$C_5H_4SiMe_2SiMe_2$) (**4•**). Strukturuntersuchungen mittels Röntgenbeugung ergaben Sandwich-Kippwinkel von 17.3° (**2•**) und 3.8° (**4•**) und beträchtliche Spannung im Ring-Brücke-Ring-Bereich. Die EPR-Spektren zeigen diese Verzerrungen an, indem der g-Tensor für **4•** tetragonal ($g_x = g_y \neq g_z$), für **2•** und **3•** hingegen rhombisch ($g_x \neq g_y \neq g_z$) ist. Mit zunehmender Kippung nimmt g geringfügig in Richtung auf g_{fs} = 2.0023 hin zu und a(^{51}V) deutlich ab. Diese Trends erklären sich aus der verzerrungsinduzierten Mischung des SOMO V($3d_{z^2}$) mit Ligand-π-Orbitalen. Während die cyclische Voltammetrie für das unverzerrte **4•** reversible Oxidation und Reduktion anzeigt, weist das gespannte [1]Trovacenophan **2•** irreversibles Redoxverhalten auf, welches sich auf die Spaltung der interannularen Brücke zurückführen läßt. [1]Silatrovacenophane sind thermisch robuster als [1]Ferrocenophane, denn **2•** bietet, auch nach thermischer Belastung auf 280°, keine Hinweise auf ringöffnende Polymerisation (ROP).

1 Introduction

Tilted sandwich complexes are of interest for a variety of reasons. With regard to electronic structure, loss of axial symmetry with attendant raising of orbital degeneracies should effect changes in spectroscopic, magnetic, and redox properties. In a different vein, the strain which is introduced by the short interannular links responsible for tilting of the sandwich backbone also modifies chemical reactivity as has been amply demonstrated by *Manners* et al. [2]. The latter have exploited this effect in the preparation of metallocene containing polymers formed by ring opening polymerization (ROP) of [1]silaferrocenophanes.

Interannular links at bis(arene)metal complexes have played an important role in our own work over the years [3]. Our recent focus on paramagnetic (η^7-tropylium)vanadium(η^5-cyclopentadienyl), trovacene **1•**, as a probe in studies of intramolecular communication initiated the plan of synthesizing tilted derivatives of parent **1•**. Apart from the fact that this type of metallocyclophane was hitherto unknown, motivation also derived from the question whether

* Prof. Dr. Ch. Elschenbroich
Fachbereich Chemie
Philipps-Universität Marburg
D-35032 Marburg/Germany
Fax: +49(0)6421/2825653
E-Mail: eb@chemie.uni-marburg.de

 DOI: 10.1002/zaac.200400247

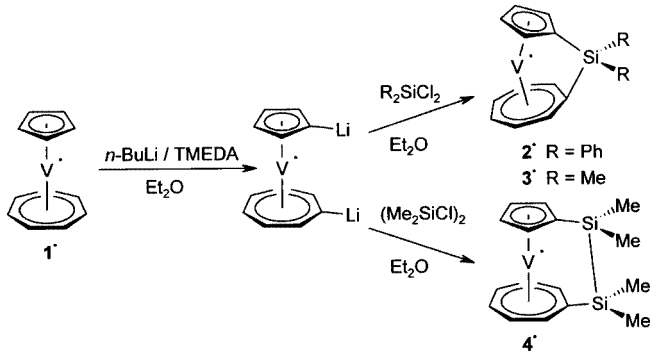

Scheme 1

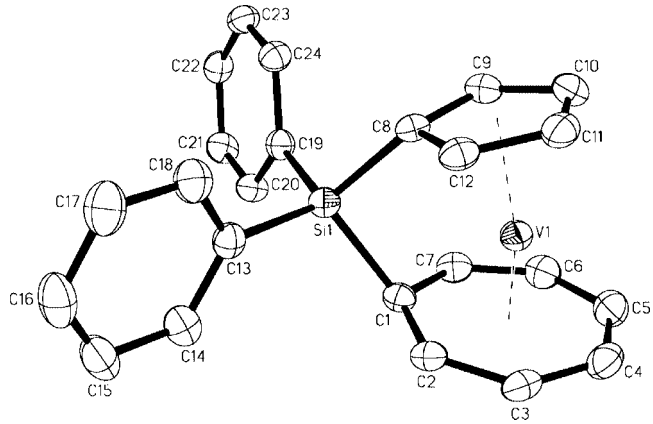

Figure 1 Molecular structure of **2•** in the crystal, SHELXTL drawing with 50 % probability ellipsoids.

tilted [1]trovacenophanes would readily undergo ROP. While [1]metallocenophanes in fact display ROP, in our hands interannularly bridged, tilted bis(arene)metal complexes failed to do so, probably for the reason that metal-ring bond-cleavage competes with polymerization [3m]. We therefore set out to prepare [1]- and [2]silatrovacenophanes, the outcome of this endeavour being reported in the sequel.

2 Results and Discussion

Synthesis

A suitable precursor in the preparation of interannularly linked trovacene derivatives would be the dilithiated species (η^7-C_7H_6Li)V(η^5-C_5H_4Li). At the start of the present study, only the monolithiated complex (η^7-C_7H_7)V(η^5-C_5H_4Li) had been obtained, however. The factors which govern reactivity, regioselectivity of monolithiation, and the control of mono- versus dilithiation of mixed sandwich complexes (η^7-C_7H_7)M(η^5-C_5H_5), M = Ti, V, Cr, still are not well understood [4]. Under mild lithiation conditions (*n*-BuLi, hexane/Et_2O, room temperature) (C_7H_7)Ti(C_5H_5) is monolithiated at η^7-C_7H_7 and (C_7H_7)V(C_5H_5) at η^5-C_5H_5. For unknown reasons, monolithiation of trovacene **1•** stops at 50 % conversion. Heteroannular dilithiation of (η^7-C_7H_7)Ti(η^5-C_5H_5) is effected by *n*-butyl lithium in the presence of *N*,*N*,*N*′,*N*′-tetramethylethylenediamine (TMEDA) [4e]. This procedure also generates (η^7-C_7H_6Li)V(η^5-C_5H_4Li), which subsequently by means of the respective organohalosilane R_2SiCl_2 can be transformed into the silatrovacenophanes 1,8-diphenylsilanediyl(η^7-cycloheptatrienyl)-(η^5-cyclopentadienyl)vanadium **2•**, 1,8-dimethylsilanediyl-(η^7-cycloheptatrienyl)(η^5-cyclopentadienyl)vanadium **3•**, and 1,8-tetramethyldisilane-1,2-diyl(η^7-cycloheptatrienyl)-(η^5-cyclopentadienyl)vanadium **4•** (Scheme I) [5]. Exhaustive heteroannular dilithiation of trovacene requires an excess of *n*-BuLi/TMEDA. In general, it is advisable to separate insoluble dilithiotrovacene by decantation before use in subsequent reactions. In the present application, however, this step proved to be superfluous, possibly because dilithiotrovacene reacts with halosilanes faster than *n*-butyllithium.

X-Ray Crystallographic Study

The structures of the [1]silatrovacenophane **2•** and the [2]silatrovacenophane **4•** are displayed in Figures 1 and 2, selected bond lengths and angles are given in Table 1. The angles describing the bending distortions are defined in Figure 3. Tilting of the sandwich axes is, of course, the prominent structural feature, it gives rise to the interplanar angles (**2•**) = 17.26(9)° and (**4•**) = 3.8(3)°, respectively. The tilt angle σ is defined as the angle of the axes connecting the two ring centroids with the central metal atom. Distortion parameters for a few related molecules are also given in Figure 3. In accordance with the larger atomic radius of vanadium, compared to chromium, interannular $-SiR_2-$ and $-GeR_2-$ links cause more extensive tilting for the vanadium sandwich complexes than for the chromium species. The effect of the size of the bridging atom is illustrated by the [1]zirconavanadarenophane **8•** which, despite the presence of a one-atom bridge, is tilted only marginally [3m]. Surprisingly, although the inter-ring distance of parent (η^7-C_7H_7)V(η^5-C_5H_5) (338 pm) is somewhat larger than in the symmetrical isomer (η^6-C_6H_6)$_2$V (322 pm), α(**2•**) falls short of α(**7•**). This must be a consequence of the disparate ring sizes in **2•**. The latter are also responsible for differing angles β_{Tr}(**2•**) and β_{Cp}(**2•**): the absence of ring slippage and identical bond distances C_1-Si and C_8-Si necessarily result in the gradation β_{Tr} (**2•**) = 45° > β_{Cp} (**2•**) = 33°.

In addition to sandwich tilting, strain also manifests itself in the deviation of the angle θ at the bridging atom E from the value appropriate for sp^3 hybridization and in the bending β of the $C_{ipso}-E$ bond vectors out of the π-perimeter planes. Chemical lability of the interannular links is therefore expected and found as will be discussed in a later section.

Structural details for the $-SiMe_2-$ bridged complex **3•** are unavailable because this material at ambient temperature is obtained as an oil which resisted all crystallization attempts.

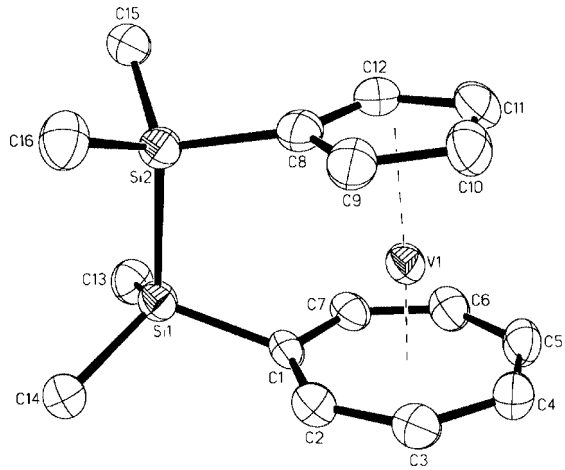

Figure 2 Molecular structure of **4•** in the crystal, SHELXTL drawing with 50 % probability ellipsoids.

Metallocene derivatives or similar ligand systems with a $-SiMe_2-SiMe_2-$ bridge are known for typical sandwich compounds with almost parallel ligand-ring arrangements (M = Cr [3d], Fe [6], Ru [7]) as well as for Cp_2TiCl_2-type complexes (M = Ti [8], Zr [8b, 9], Hf [10]). The Si−Si distance for the first mentioned type of compound can vary between 233.4(8) and 237.0(2) pm [6d, 7] depending on the steric conditions generated by the metals and the aromatic ligand system. The value of 235.5(2) pm in **4•** fits into this range. For the latter type of complex usually a somewhat shorter Si−Si bond was observed caused by the reduced steric stress in the pseudo-tetrahedral environment. Typical values lie between 232.4(3) and 233.1(3) pm [8b].

Electron Paramagnetic Resonance

EPR spectroscopy has proved to be an invaluable tool in the study of $V^0(d^5)$ sandwich complexes. While for oligonuclear V^0 complexes ^{51}V hyperfine analysis reveals intramolecular magnetic interaction [11], in the case of mononuclear derivatives substituent effects and structural distortions are assessed [3]. With regard to the silatrovacenes **2•-4•**, which form the topic of the present investigation, the effect of tilting on g- and hyperfine anisotropy are at stake. Rigid solution EPR spectra of **2•** and **4•** are depicted in Figure 4, the data are collected in Table 2. As expected, the spectral record for **4•** (α = 3.8°) closely matches that observed for parent **1•** (α = 0°); the small changes of the parameters <g>, $a(^{51}V)$, $g_{\parallel}$, $g_{\perp}$, $A_{\parallel}(^{51}V)$, and $A_{\perp}(^{51}V)$ reflect the weakly electron withdrawing nature of organosilyl substitution in **4•**. Even for the more extensively tilted complex **2•** (α = 17.3°), loss of axial symmetry is barely resolved in the rigid solution X-band EPR spectrum; resort to Q-band measurements was therefore taken, which form the basis for the data collected in Table 2. Inspection of the parameters extracted for the species **1•**, **2•**, and **4•** reveals that <g> increases and $a(^{51}V)$ decreases with increasing tilt. The same gradation had been observed previously for the couple $\mathbf{11}^{\ddagger}$

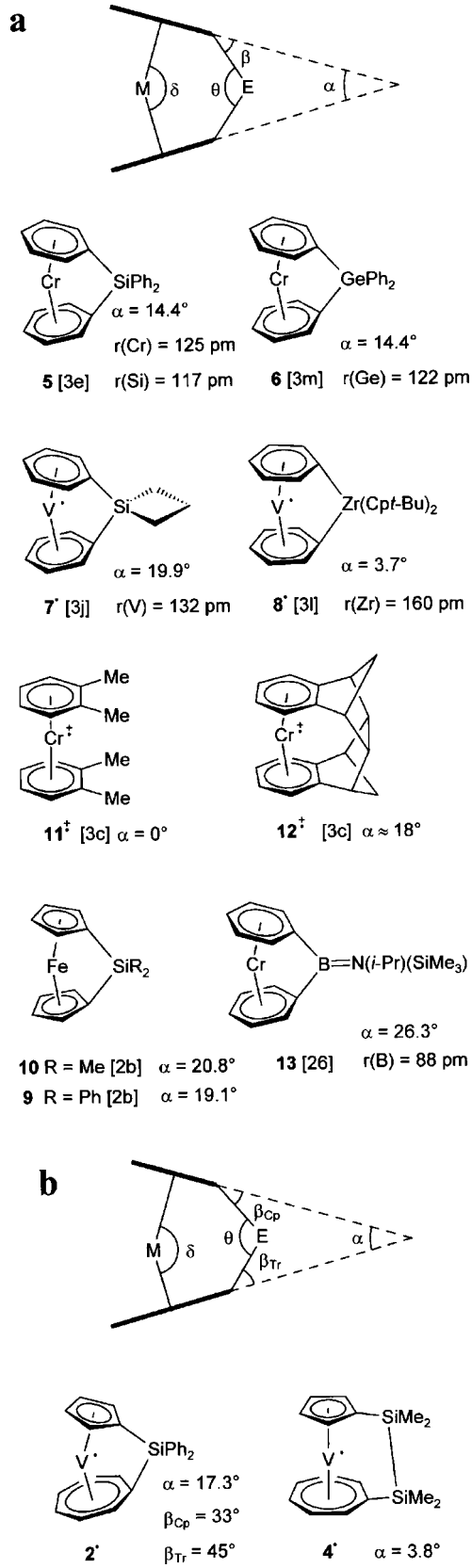

Figure 3 Schematics of interannularly bridged symmetrical (a) and unsymmetrical (b) sandwich complexes and designations of the relevant angles which describe the distortions: **2•**, **4•** (this paper) and **5-12** (as reported previously).

Table 1 Selected bond lengths/pm and bond angles/° in **2**• and **4**•[a)]

		2•			
V1···Si1	288.00(7)	C1−Si1−C8	98.17(8)	C13−Si1−C19	111.67(9)
V1−C1	213.6(2)	C1−Si1−C13	111.69(9)	C1−Si1−C19	113.58(8)
V1−C2	216.3(2)	C8−Si1−C13	110.88(8)	C8−Si1−C19	110.11(9)
V1−C3	220.6(2)	Si1−C1−C2	111.6(1)	Si1−C1−C7	110.1(1)
V1−C4	221.0(2)	C2−C1−C7	124.2(2)	C1−C2−C3	130.1(2)
V1−C5	220.3(2)	C2−C3−C4	129.4(2)	C3−C4−C5	128.0(2)
V1−C6	220.3(2)	C4−C5−C6	127.7(2)	C5−C6−C7	130.0(2)
V1−C7	217.8(2)	C1−C7−C6	129.8(2)	Si1−C8−C9	121.8(1)
V1−C8	221.6(2)	Si1−C8−C12	120.7(1)	C9−C8−C12	105.0(2)
V1−C9	223.2(2)	C8−C9−C10	109.4(2)	C9−C10−C11	108.4(2)
V1−C10	227.3(2)	C10−C11−C12	107.5(2)	C11−C12−C8	109.7(2)
V1−C11	228.4(2)				
V1−C12	224.0(2)				
Si1−C1	188.9(2)	Si1−C8	187.7(2)	Si1−C13	186.6(2)
Si1−C19	186.3(2)	C1−C2	143.6(3)	C1−C7	143.5(3)
C2−C3	141.4(3)	C3−C4	140.9(3)	C4−C5	140.9(3)
C5−C6	141.0(3)	C6−C7	140.9(3)	C8−C9	143.6(3)
C8−C12	144.0(3)	C9−C10	141.0(3)	C10−C11	141.3(3)
C11−C12	141.1(3)				
		4•			
V1−C1	219.1(4)	C1−Si1−Si2	102.9(1)	C8−Si2−Si1	105.4(2)
V1−C2	219.1(5)	Si1−C1−C2	115.6(3)	Si1−C1−C7	116.3(3)
V1−C3	218.9(6)	C2−C1−C7	125.9(4)	C1−C2−C3	129.7(5)
V1−C4	219.6(6)	C2−C3−C4	128.8(6)	C3−C4−C5	128.1(6)
V1−C5	219.9(5)	C4−C5−C6	128.5(6)	C5−C6−C7	129.6(6)
V1−C6	219.4(5)	C6−C7−C1	129.3(5)	Si2−C8−C9	126.2(5)
V1−C7	219.1(5)	Si2−C8−C12	126.2(5)	C9−C8−C12	107.2(5)
V1−C8	226.2(6)	C8−C9−C10	109.0(6)	C9−C10−C11	107.1(6)
V1−C9	226.7(6)	C10−C11−C12	108.0(6)	C11−C12−C8	108.7(6)
V1−C10	226.7(6)				
V1−C11	226.6(6)				
V1−C12	225.5(6)				
Si1−Si2	235.5(2)	Si1−C1	189.4(6)	Si2−C8	189.0(6)
C1−C2	143.3(7)	C1−C7	143.1(7)	C2−C3	141.0(8)
C3−C4	143.1(8)	C4−C5	140.5(9)	C5−C6	140.4(9)
C6−C7	141.6(8)	C8−C9	141.9(8)	C8−C12	141.4(8)
C9−C10	142.9(9)	C10−C11	142(1)	C11−C12	143(1)

[a)] Further details can be obtained from the Cambridge Crystallographic Data Center, 12 Union Road, Cambridge CB2 1EZ by quoting the numbers CCDC 237109 and CCDC 237110 (Fax: (+44) 1223-3 36-0 33; e-mail: deposit@ccdc.cam.ac.uk).

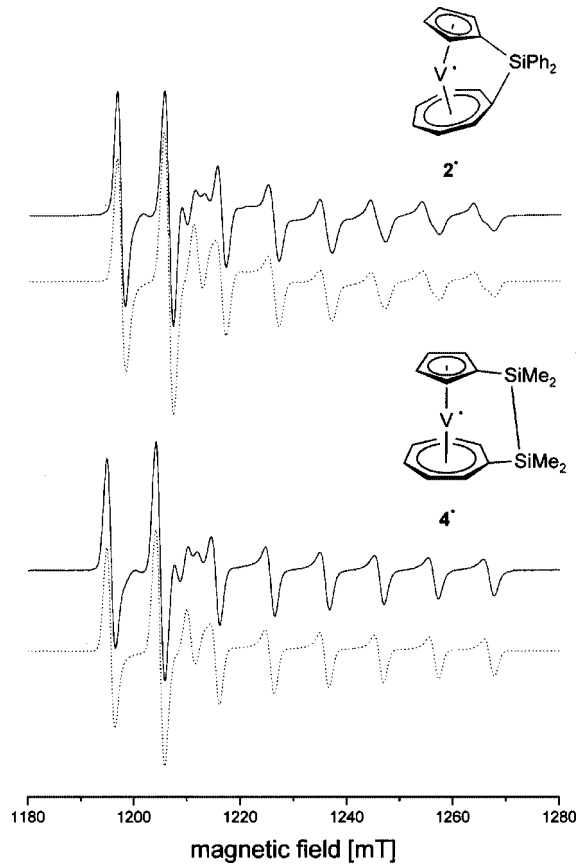

Figure 4 EPR spectra of **2**• and **4**• in rigid solution (toluene, 110 K; Q band ν = 34.0137 GHz)
Experimental (—) and simulated (····)

Table 2 EPR parameters for axially symmetric **1**• and tilted **2**• and **4**•.

	1•	**4**•	**2**•
α	0°	3.8°	17.3°
g_{iso}	1.9815	1.9816	1.9832
g_1		1.9724	1.9737
g_2 [$g_\perp$]	1.9725	1.9718	1.9715
g_3 [$g_\parallel$]	1.9994	1.998	1.9993
<g> (calcd)	1.9815	1.9813	1.9815
a(^{51}V)/mT	7.20	7.03	6.76
A_1(^{51}V)/mT	10.26	10.19	9.62
A_2(^{51}V) [$A_\perp$(^{51}V)]/mT	10.37	10.36	10.08
A_3(^{51}V) [$A_\parallel$(^{51}V)]/mT	0.97	0.53	0.6
<A(^{51}V)> (calcd)/mT	7.20	7.03	6.76

(α = 0°) and **12**$^{+}$ (α = 18°), which features Cr^{+}(d^5) instead of V•(d^5) as the central metal [3c]. The inverse response of <g> and a(^{51}V) to tilting suggests that this distortion is accompanied by a slight increase in metal→ligand spin delocalization, which would serve to reduce the spin-orbit coupling contribution to the g factor and the extent of central metal hyperfine coupling. Axially symmetric bis(arene)-metal(d^5) sandwich complexes possess the frontier orbital sequence $e_2^4a_1^1e_1^0$. The SOMO a_1 is an essentially non bonding M(d_{z^2}) function, metal ligand overlap being almost nil because the ligand π-orbitals are positioned in the nodal plane of the M(d_{z^2}) orbital. This situation changes upon tilting distortion, a modified molecular orbital diagram for bent metallocenes has been proposed by *Green* [12] and refined by *Hoffmann* [13]. Accordingly, the degeneracies of the e_2- and e_1 levels are raised and the new sequence $1a_1b_2 2a_1b_1a_2$ emerges [13], in which the SOMO $2a_1$ can now mix with $1a_1$. Since $1a_1$ is of e_2 origin (δ-bonding in the undistorted sandwich), mixing of metal-dominated $2a_1$ with $1a_1$ is expected to cause a decrease of spin density on the central metal atom and a reduction of hyperfine coupling as actually observed for tilted **2**•. It is worth mentioning that the extent of δ-backbonding from filled metal d_{xy} and $d_{x^2-y^2}$ orbitals to unoccupied ligand orbitals increases with increasing π-perimeter size. Therefore, the composition $(C_7H_7)M(C_5H_5)$ should be comparable to $(C_6H_6)M(C_6H_6)$, where bonding is thought to be dominated by the $M\overset{\delta}{\rightarrow}C_nH_n$ contribution [14].

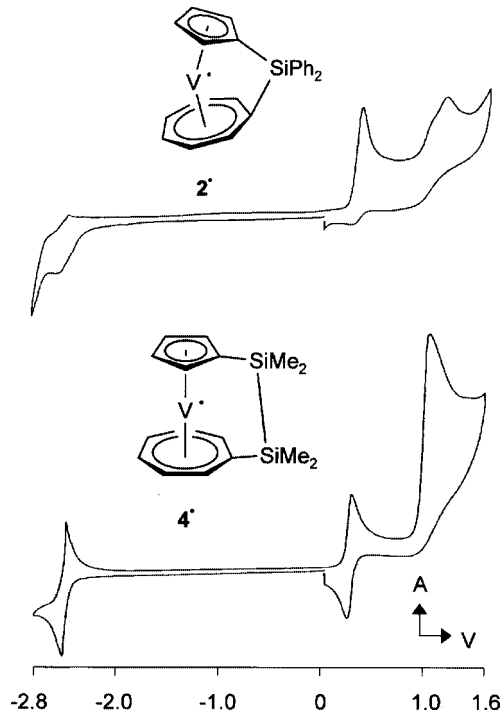

Figure 5 Cyclic voltammograms for **2•** and **4** in DME/*n*-Bu_4NClO_4 at −40 °C and 100 mV/s vs. SCE. Compound **2**: $E_{pa}(+/0)$[a] = 0.376 V; $E_{1/2}(0/-) = -2.473$ V, $\Delta E_p = 41$ mV, $r = 1$. Compound **4**: $E_{1/2}(+/0) = 0.260$ V, $\Delta E_p = 76$ mV, $r = 1$; $E_{1/2}(0/-) = -2.489$ V, $\Delta E_p = 66$ mV, $r = 1$. Compound **1** [10]: $E_{1/2}(+/0) = 0.260$ V, $\Delta E_p = 64$ mV, $r = 0.9$; $E_{1/2}(0/-) = -2.55$ V, $\Delta E_p = 66$ mV, $r = 1$. [a]Irreversible process.

Redox properties

Parent trovacene **1•** undergoes two reversible redox processes, which according to cyclic voltammetry (CV *vs* SCE) proceed at the potentials $E_{1/2}(+/0) = +0.26$ V and $E_{1/2}(0/-) = -2.55$ V [15]. Again, as in the case of the EPR spectra, the weakly tilted complex **4•** mimicks parent **1•** whereas the strongly tilted complex **2•** differs in that oxidation is irreversible and reduction is ill defined. The CV traces for **2•** and **4•** are shown in Figure 5, electrochemical data are found in the respective captions. The observation that the redox potentials of **4•** are almost the same as those of **1•** may be explained by the fact that in **4•** the anodic shift typical for silyl substitution is compensated by $Si-Si(\sigma)|\eta^n\text{-}C_nH_n(\pi)$ conjugation. The latter should be particularly effective in the [2]silatrovacenophane structure since the Si−Si σ-bond vector is parallel to the axes of the π-perimeter ligand orbitals. Precedent for the electrochemical behavior of **2•** exists with the complexes **5•** [3e], **6•** [3m], and **7•** [3j], which also display totally irreversible oxidation. In view of the well-known sensitivity of the η^6-arene-Si bond to solvodesilylation [16], the strain inherent in the one-atom *ansa*-sandwich structure and the higher susceptibility of cations to nucleophilic attack, the ready cleavage of the one-atom interannularly bridges in **2•** and **5•**-**7•** during electrochemical oxidation is not surprising. This picture also serves to rationalize the more robust nature of **4•** under oxidizing and reducing conditions (absence of strain) and of **2•** and **5•**-**7•** under reducing conditions (attenuation of susceptibility to nucleophilic attack).

Experiments Directed at Ring Opening Polymerization (ROP)

Chemically induced cleavage of the interannular link in [1]silametallocenophanes is complemented by thermal ring opening, which can lead to macromolecules in which 1,1′-metallocenediyl units alternate with $-SiR_2-$ groups [2]. It therefore was of interest to inquire whether this type of ring opening polymerization also proceeds with [1]silatrovacenophanes **2•** and **3•**. An attractive feature of this system is the fact that a silyltrovacenyl based organometallic polymer would contain a paramagnetic repeating unit which would trigger questions of magnetic coupling along this polyradical chain. Spin exchange is expected to profit from the known ability of organosilanes to promote conjugation [17]. In fact, we have previously observed antiferromagnetic exchange in dinuclear bis(η^6-benzene)vanadium derivatives, mediated by organosilicon spacers [3i]. Even in the case of a disilyl spacer, the exchange coupling constant J exceeded the value of the hyperfine coupling constant a(^{51}V) by a factor of 100, which renders exchange moderately strong on the ^{51}V hyperfine scale still keeping it in a range where it noticeably shapes the hyperfine pattern.

Since the $-SiMe_2-$ bridged complex **3•** could not be fully characterized as a pure material, thermolysis experiments were inconclusive. EI-MS mass spectrometric analysis pointed to the presence of the trimer $TVC-SiMe_2-TVC-SiMe_2-TVC$ together with the target molecule **3•**. However, it is not clear whether the trimer arose during the synthesis in a reaction competing with [1]silatrovacenophane formation or whether it constitutes a ring opening oligomerization product generated during the EI-MS experiment. The latter alternative gains some support from the observation that the initial product in the synthesis of **3•** furnishes an EPR spectrum which advocates the presence of mononuclear TVC derivatives only, whereas after heating to 80 °C in the presence of a trace of $PtCl_2$ for 2 h, the EPR spectrum of a dinuclear trovacene derivative is superimposed on the monomer spectrum (Figure 6a). Pt catalyzed ROP has been reported for the [1]silaferrocenophane **10** [2c].

Dimers, trimers, and possibly oligomers comprised of the units $-TVC-SiMe_2-$ are also found if the synthesis is carried out in refluxing tetrahydrofuran. In different runs of this experiment, the respective products displayed EPR spectra which attest to the presence of exchange coupled dinuclear [15 lines, splitting a(^{51}V, **1•**)/2] and trinuclear [22 lines, splitting a(^{51}V, **1•**)/3] trovacene derivatives (Figure 6b). Again, it is not apparent whether the latter are formed initially or whether they are the products of secondary ring opening.

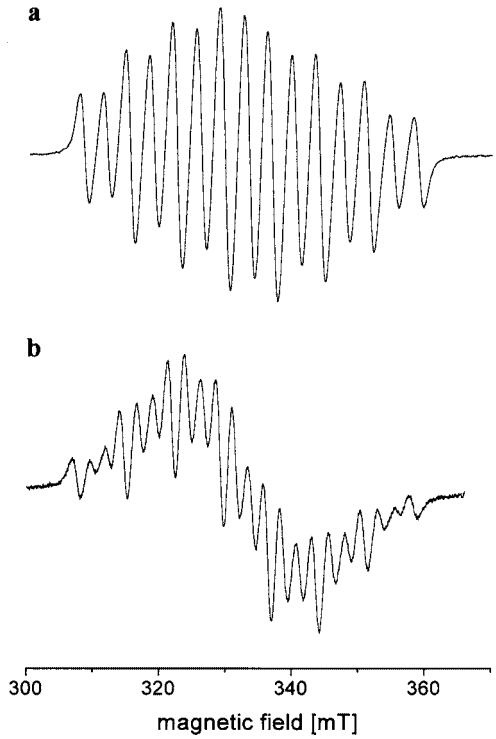

Figure 6 EPR spectra (X band, 298 K) of solutions obtained during attempted ring opening polymerization (ROP); **a 3•** in toluene, trace of $PtCl_2$, 80 °C for 2h; **b 3•** in THF, reflux for 8 h. The observation of 15 and 22 line ^{51}V hyperfine patterns displaying splittings one half and one third of that of monomeric **3•** attest to the presence of exchange coupled diradicals and triradicals, respectively, in solution.

Table 3 Crystallographic data of **2•** and **4•**

instrument	IPDS II (Stoe)	IPDS II
radiation	Mo-K_α	Mo-K_α
formula	$C_{24}H_{20}SiV$	$C_{16}H_{22}Si_2V$
formular weight/g·mol	387.45	321.47
crystal size/mm	0.23×0.20×0.08	0.40×0.34×0.12
a/pm	1114.3(2)	664.0(1)
b/pm	1527.0(2)	1310.9(1)
c/pm	1190.7(2)	944.8(1)
β/°	111.91(1)	104.72(1)
unit cell volume/10^6 pm^3	1879.7(5)	795.4(2)
Z	4	2
d_{calc}	1.369	1.342
crystal system	monoclinic	monoclinic
space group (No.)	$P2_1/n$ (14 [22])	$P2_1$
absorption correction	numerical	numerical
μ/cm^{-1}	6.0	7.6
temperature/K	193	193
$2\theta_{max}$/°	52.51	52.37
hkl values	$-13 \le h \le 13$ $-18 \le k \le 18$ $-14 \le l \le 14$	$-8 \le h \le 8$ $-18 \le k \le 18$ $-14 \le l \le 14$
measured reflection	26752	11497
unique reflections	3770	3064
R_{int}	0.0668	0.0731
reflections with $F_o > 4\sigma(F_o)$	2544	2917
parameter	315	217
structure solution	direct methods (SIR-92 [23])	direct methods (SHELXS-97 [24])
refinement against F^2	− SHELXL-97 [25] −	
H atoms	a)	a)
Flack-Parameter	−	0.02(4)
R_1	0.0284	0.0631
wR_2 (all data)	0.0604[b]	0.1755[c]
max. residual electron density /10^{-6} e·pm^3	0.26	1.57

[a] Free refinement. [b] $w = 1/[\sigma^2(F_o^2)+(0.0323\cdot P)^2]$; $P = [\max(F_o^2, 0)+2\cdot F_c^2]/3$. [c] $w = 1/[\sigma^2(F_o^2)+(0.1297\cdot P)^2+(0.32\cdot P)]$.

[1]Silaferrocenophane **9** bearing an $-SiPh_2-$ interannular link was shown to engage in quantitative ring opening polymerization, albeit at higher temperature than the $-SiMe_2-$ analogue [2]. Contrarily, in our hands the $-SiPh_2-$ bridged [1]trovacenophane **2•** fails to undergo ROP even at 280 °C since, after thermal treatment, MS- und EPR analysis revealed the presence of the unchanged monomer **2•**. It may therefore be concluded that [1]silatrovacenophanes are considerably more robust than [1]silaferrocenphanes, which is surprising in view of the fact that the tiltingangles differ only marginally. More extensive steric shielding of the silicon atom in **2•**, compared to **3•** and **4•**, comes to mind as an explanation for the more robust nature of **2•**. Possibly, a two component ROP, utilizing **3•** and **10**, will lead to organometallic polymers in which a $(-C_5H_4)Fe(C_5H_4-SiMe_2-)$ backbone is interspersed with paramagnetic $(-C_7H_6)V(C_5H_4-SiMe_2-)$ units. This approach had been chosen to incorporate $(-C_6H_5)Cr(C_6H_5-SiMe_2-)$ blocks into a polysilaferrocenophane chain [19] while neat [1]silachromarenophanes **5** failed to yield a ROP product.

Experimental Section

Chemical manipulations and physical measurements were performed using standard techniques and instruments specified previously [18]. Trovacene $(\eta^7\text{-}C_7H_7)V(\eta^5\text{-}C_5H_5)$ (**1•**) was prepared as described in the literature [20].

X-ray data collection

The crystals were covered with a perfluorinated polyether and mounted at the top of a glass capillary under a flow of cold gaseous nitrogen. The reflection were collected with a IPDS II diffractometer (Stoe; λ = 71.073 pm). The intensities were corrected for Lorentz and polarization effects (for absorption correction, cell parameters, and collecting of the intensities, see Table 3). **4•** crystallizes in the Sohncke space group $P2_1$ [21]. Transformation in $P2_1/m$ is not possible (see also Flack-Parameter in Table 1). Selected bond lengths and angles of **2•** and **4•** are listed in Table 1.

$(\eta^7\text{-}\overline{C_7H_6})V(\eta^5\text{-}C_5H_4\overline{SiPh_2})$ (2•). A 100 mL flask equipped with a magnetic stirring bar was charged with (η^7-cycloheptatrienyl)-(η^5-cyclopentadienyl)vanadium (0.20 g, 0.97 mmol), diethyl ether (30 mL), and *N*,*N*,*N*′,*N*′-tetramethylethylenediamine (TMEDA) (0.58 mL, 3.83 mmol). *n*-BuLi (2.41 mL, 3.83 mmol, solution 1.6 M in hexane) was added dropwise and the mixture was refluxed for 4 h. After cooling to −20 °C dichlorodiphenylsilane (0.2 mL, 0.97 mmol) dissolved in petroleum ether (10 mL) was added during 2 h to the dark-violet suspension. The color of the mixture turned from dark-brown to violet and LiCl precipitated. The mixture was stirred at room temperature overnight. Filtration and storing of the solution at −20 °C yielded violet crystals which were suitable for X-ray diffraction.

Yield: 0.24 g, 64 %.
Elemental analysis: $C_{24}H_{20}SiV$ (387.45): calcd C 74.70, H 5.20; found C 73.14, H 5.78 %.
EI-MS (70 ev) m/z = 387 [M^+] (100 %); 309 [M^+-Ph] (14 %); 232 [M^+-2Ph] (14 %); 205 [M^+-$SiPh_2$] (3 %).

(η^7-C_7H_6)V(η^5-$C_5H_4SiMe_2SiMe_2$) (4'). The preparation was carried out in analogy to that of **2'**, this time using (η^7-C_7H_7)V(η^5-C_5H_5) (0.15 g, 0.72 mmol), TMEDA (0.43 mL, 2.88 mmol), *n*-BuLi (1.81 mL, 2.88 mmol, sol. 1.6 M in hexane), 1,2-dichlorotetramethyldisilane (0.13 mL, 0.72 mmol).
Yield: 0.10 g, 45 %.
Elemental analysis: $C_{16}H_{22}Si_2V$ (321.46): calcd C 59.78, H 6.90; found C 56.83, H 7.04. EI-MS (70 eV) m/z = 321 [M^+] (9 %); 205 [M^+-Si_2Me_4] (37 %); 116 [$C_5H_5V^+$] (54 %); 91 [$C_7H_7^+$] (20 %).

(η^7-C_7H_6)V(η^5-$C_5H_4SiMe_2$) (3'). The synthesis of **3'** was attempted in the same way as that of **2'**, replacing Ph_2SiCl_2 by Me_2SiCl_2 (0.12 mL, 0.97 mmol), dissolved in petroleum ether (10 mL). The product was a violet oil which resisted further purification. Column chromatography led to deposition of insoluble material. Heating to 150 °C for 1 h in an evacuated tube resulted in no visible change. Microanalysis revealed a small content (≈ 3 %) of nitrogen, which points to coordinated TMEDA. EI-MS (70 eV) m/z = 734 [TVC−$SiMe_2$−TVC−$SiMe_2$−TVC] (50 %); 264 [**3**$^+$] (15 %); 207 [TVC^+] (2 %); 91 [$C_7H_7^+$] (100 %).

Acknowledgement. This work was supported by the Volkswagen-Stiftung, the Deutsche Forschungsgemeinschaft, and the Fonds der Chemischen Industrie. We thank Tina Schmidt for technical assistance.

References

[1] Ph. D. Thesis, F. Paganelli, Marburg (2003). Part 9: Ch. Elschenbroich, J. Plackmeyer, M. Nowotny, K. Harms, J. Pebler, *Inorg. Chem*., submitted.
Trovacene = (η^7-**tro**pylium)**va**nadium(η^5-**c**yclop**en**tadienyl). The number in brackets indicates the site of peripheral substitution: [7]trovacenyl derivatives are functionalized at the cycloheptatrienyl ligand, [5]derivatives at the cyclopentadienyl ligand.

[2] a) D. A. Foucher, B.-Z. Tang, I. Manners, *J. Am. Chem. Soc*. **1992**, *114*, 6246; b) I. Manners, *Adv. Organomet. Chem*. **1995**, *37*, 131; c) P. Nguyen, P. Go´mez-Elipe, I. Manners, *Chem. Rev.* **1999**, *99*, 1515.

[3] a) Ch. Elschenbroich, F. Stohler, *Chimia* **1974**, *28*, 730; b) Ch. Elschenbroich, R. Möckel, U. Zenneck, *Angew. Chem.* **1978**, *90*, 560; *Angew. Chem. Int. Ed. Engl.* **1978**, *17*, 531; c) Ch. Elschenbroich, J. Schneider, H. Prinzbach, W.-D. Fessner, *Organometallics* **1986**, *5*, 2091; d) Ch. Elschenbroich, J. Hurley, W. Massa, G. Baum, *Angew. Chem.* **1988**, *100*, 727; *Angew. Chem. Int. Ed. Engl.* **1988**, *27*, 684; e) Ch. Elschenbroich, J. Hurley, B. Metz, W. Massa, G. Baum, *Organometallics* **1990**, *9*, 889; f) Ch. Elschenbroich, E. Bilger, B. Metz, *Organometallics* **1991**, *10*, 2823; g) Ch. Elschenbroich, J. Sebbach, B. Metz, G. Heikenfeld, *J. Organomet. Chem.* **1992**, *426*, 173; h) M. Nowotny, Ch. Elschenbroich, A. Behrendt, W. Massa, S. Wocadlo, *Z. Naturforsch.* **1993**, *48b*, 1581; i) Ch. Elschenbroich, A. Bretschneider-Hurley; J. Hurley, W. Massa, S. Wocadlo, J. Pebler, *Inorg. Chem*. **1993**, *32*, 5421; j) Ch. Elschenbroich, B. Metz, B. Neumüller, E. Reijerse, *Organometallics* **1994**, *13*, 5072; k) Ch. Elschenbroich, A. Bretschneider-Hurley, J. Hurley, A. Behrendt, W. Massa, S. Wocadlo, E. Reijerse, *Inorg. Chem.* **1995**, *34*, 743; l) Ch. Elschenbroich, Th. Isenburg , A. Behrendt, *Inorg. Chem*. **1995**, *34*, 6565; m) Ch. Elschenbroich, E. Schmidt, B. Metz, K. Harms, *Organometallics* **1995**, *14*, 4043; n) Ch. Elschenbroich, E. Schmidt, R. Gondrum, B. Metz, O. Burghaus, W. Massa, S. Wocadlo, *Organometallics* **1997**, *16*, 4589.

[4] a) C. J. Groenenboom, H. J. de Liefde Meijer, F. Jellinek, *Rec. Trav. Chim. Pays-Bas* **1974**, *93*, 6; b) C. J. Groenenboom, H. J. de Liefde Meijer, F. Jellinek, *J. Organomet. Chem*. **1974**, *69*, 235; c) C. J. Groenenboom, F. Jellinek, *J. Organomet. Chem*. **1974**, *80*, 229; d) M. Vliek, C. J. Groenenboom, H. J. de Liefde Meijer, F. Jellinek, *J. Organomet. Chem*. **1975**, *97*, 67; e) L. B. Kool, M. Ogasa, M. D. Rausch, R. D. Rogers, *Organometallics* **1989**, *8*, 1785; f) M. Ogasa, M. D. Rausch, R. D. Rogers, *J. Organomet*. *Chem.* **1991**, *403*, 279; g) M. L. H. Green, D. K. P. Ng, *Chem. Rev.* **1995**, *95*, 439; h) N. Kaltsoyannis, *J. Chem. Soc., Dalton Trans.* **1995**, 3727; i) For the electron-density distribution in mixed sandwiches (η^7-C_7H_7)M(η^5-C_5H_5), M = Ti, V, Cr, see K. A. Lyssenko, M. Yu. Antipin, S. Yu. Ketkov, *Russ. Chem. Bull., Int. Ed*. **2001**, *50*, 130.

[5] F. Paganelli, *PhD Thesis*, Univ. Marburg 2003.

[6] a) P. Jutzi, R. Krallmann, G. Wolf, B. Neumann, H.-G. Stammler, *Chem. Ber.* **1991**, *124*, 2391; b) W. Finckh, B.-Z. Tang, D. A. Foucher, D. B. Zamble, R. Ziembinski, A. Lough, I. Manners, *Organometallics* **1993**, *12*, 823; c) V. V. Dement'ev, F. Cervantes-Lee, L. Parkanyi, H. Sharma, K. H. Pannell, M. T. Nguyen, A. Diaz, *Organometallics* **1993**, *12*, 1983; d) T. J. Peckham, D. A. Foucher, A. J. Lough, I. Manners, *Can. J. Chem.* **1995**, *73*, 2069.

[7] J. M. Nelson, A. J. Lough, I. Manners, *Organometallics* **1994**, *13*, 3703.

[8] a) S.-S. Xu, X.-B.Deng, B.-Q. Wang, X.-Z. Zhou, *Acta Chim. Sinicia* **1997**, *55*, 829; b) G. Tian, B. Wang, S. Xu, Y. Zhang, X. Zhou, *J. Organomet. Chem.* **1999**, *579*, 24; c) X.-L. Sun, B.-Q. Wang, S.-S. Xu; X.-Z. Zhou, J. Zhao, Y.-L. Hu, *Chem. J. Chin. Uni.* **2000**, *21*, 222.

[9] a) Y. Wang, X. Zhou, X. Yao, H. Wang, *Chem. J. Chin. Uni.* **1991**, *12*, 488; b) K.-H. Thiele, Ch. Schliessburg, K. Baumeister, K. Hassler, *Z. Anorg. Allg. Chem.* **1996**, *622*, 1806; c) O. Perez-Camacho, S. Y. Knjazhanski, G. Cadenas, M. J. Rosales-Hoz, M. A. Leyva, *J. Organomet. Chem.* **1999**, *585*, 18; d) P. Biagini, G. P. Borsotti, G. Lugli, A. M. Romano, R. Santi, R. Millini, *J. Chem. Cryst.* **2000**, *30*, 699.

[10] X.-Z. Zhou, Y. Wang, S.-S. Xu, H.-G. Wang, X.-K. Yao, *Chem. Res. Chin. Uni.* **1992**, *8*, 239.

[11] Ch. Elschenbroich, M. Wolf, J. Pebler, K. Harms, *Organometallics* **2004**, *23*, 454, and previous papers in the series.

[12] a) J. C. Green, M. L. H. Green, C. K. Prout, *J. Chem. Soc. Chem. Comm*. **1972**, 421; b) M. L. H. Green, *Pure Appl. Chem.* **1972**, *30*, 373; c) J. C. Green, S. E. Jackson, B. Higginson, *J. Chem. Soc. Dalton Trans.* **1975**, 403.

[13] J. W. Lauher, R. Hoffmann, *J. Am. Chem. Soc*. **1976**, *98*, 1729.

[14] a) W. A. King, S. Di Bella, G. Lanza, K. Khan, D. J. Duncalf, F. G. N. Cloke, I. L. Fragala, T. J. Marks, *J. Am. Chem. Soc*. **1996**, *118*, 627; b) V. M. Rayo´n, G. Frenking, *Organometallics* **2003**, *22*, 3304; Ch. Elschenbroich, *Organometallchemie*, 4. Aufl., Teubner, Wiesbaden 2003, p. 496.

[15] Ch. Elschenbroich, E. Bilger, B. Metz, *Organometallics* **1991**, *10*, 2823.

[16] Ch. Elschenbroich, *J. Organomet. Chem*. **1970**, *22*, 677.

[17] R. D. Miller, J. Michl, *Chem. Rev.* **1989**, *89*, 1359.

[18] Ch. Elschenbroich, E. Schmidt, B. Metz, W. Massa, S. Wocadlo, O. Burghaus, *Z. Anorg*. *Allg. Chem*. **1999**, *625*, 875.

[19] K. C. Hultzsch, J. M. Nelson, A. J. Lough, I. Manners, *Organometallics* **1995**, *14*, 5496.
[20] a) R. B. King, F. G. A. Stone, *J. Am. Chem. Soc*. **1959**, *81*, 5263; b) C. Floriani, *J. Chem. Soc. Dalton Trans.* **1976**, 1046.
[21] H. D. Flack, *Helv. Chim. Acta* **2003**, *86*, 905.
[22] *International Tables for Crystallography*, 2. Aufl., Kluwer Academic Publishers, Dordrecht, 1989, Bd. A.
[23] A. Altomare, G. Cascarano, C. Giacovazzo, A. Guagliardi, M. C. Burla, G. Polidori, M. Camalli, *SIR-92*, Bari, Perugia, Rom, 1992.
[24] G. M. Sheldrick, *SHELXS-97*, Göttingen, 1997.
[25] G. M. Sheldrick, *SHELXL-97*, Göttingen, 1997.
[26] H. Braunschweig, M. Homberger, C. Hu, X. Zheng, E. Gullo, G. Clentsmith, M. Lutz, *Organometallics* **2004**, *23*, 1968.

